Journal of Power Sources 190 (2009) 121–132

Contents lists available at ScienceDirect

Journal of Power Sources

journal homepage: www.elsevier.com/locate/jpowsour

Increase of the fuel cell system efficiency — Modular testing, analysis and development environment

P. König*, E. Ivers-Tiffée

Institut für Werkstoffe der Elektrotechnik IWE, Universität Karlsruhe (TH), Karlsruhe 76131, Germany

ARTICLE INFO

Article history:
Received 6 May 2008
Received in revised form 6 July 2008
Accepted 19 July 2008
Available online 26 July 2008

Keywords:
Fuel cell system
Simulation
Standardised testing

ABSTRACT

The main issue in preparing fuel cell systems for the future market is system reliability and efficiency. Apart from successful field test trials, any type of stationary, in general automotive or portable fuel cell systems are at the development stage. One task to deal with is to increase the component and system efficiencies by facilitating the system construction or eliminating parasitic components.With newly established effective standardised system and component tests, linked with a flexible modelling and simulation environment, the development process and the determination of the system efficiencies as well as the inaccessible system values can be accelerated.In this work a modular model-aided system analysis and development environment is presented which has been evaluated and validated at the IWE. The tool, a combination of standardised testing, modelling and simulation, has been applied to different types of fuel cell systems showing the tool flexibility, modularity and accuracy. In the presented case the tool was used for system analysis and studies on efficiency increase of a complex prototype stationary PEMFC system.

1. Introduction

Standardised testing, modelling and simulation play key roles in the improvement of fuel cell systems and applications. The sole realisation of hardware tests for system analysis and improvement is not enough, often takes too long or is even impossible. During system testing many important values and a plurality of parameters necessary for a detailed analysis or even an exact comparison of different systems are not accessible. As a consequence, standardised testing has to be linked with modelling and simulation (Fig. 1), aiming for additional component and system information and a reduction of measurements. The limited number of standard test routines will therefore deliver the necessary model parameters.

At the IWE a model-aided testing and simulation approach has been evaluated [1,2] and extended to fit all kinds of fuel cell systems. For validation purposes and to show the tool flexibility, modularity and accuracy for a wide range of applications it has been applied to a complex prototype stationary a 2 kW_{el} and 4 $kW_{thermal}$ PEMFC Combined Heat and Power (CHP) system *EDISon* [1–3] (Fig. 2), a 1 kW_{el} commercial methanol-based PEMFC Auxiliary Power Unit (APU) and a fictive stationary 1 kW_{el} SOFC CHP system [4].

In this work the tool was used for a more detailed analysis of the prototype stationary 2 kW_{el} PEMFC system *EDISon*. The results of the performed studies on possible efficiency increase by system design improvement and optimised system operation are shown.

2. Standardised system testing

Aside the reduction of system tests it is a main task to standardise them in order to get comparable system test results and to determine additional interesting system parameters for the system and component models. Therefore a harmonised testing format has been developed. During the European Commission funded project FCTESTNET [5] test module programs have been evaluated based on existing IWE testing experience with stationary systems [3] or APU systems as well as international codes and standards (Fig. 3). These test modules are going to be further proofed in the European Commission funded project FCTESQA [6].

3. Flexible modelling and simulation environment

For system development and design, many companies and research institutes use models which fit their in-house development. But for an effective system improvement models are required flexible to fit with a wide variety of system types. A further important attribute of a system modelling and simulation tool is its ability to perform dynamic and transient simulation studies by providing additionally an easy to handle functionality.

At the Universität Karlsruhe (TH), Institut für Werkstoffe der Elektrotechnik (IWE) a flexible and easy to handle dynamic model-

* Corresponding author. Tel.: +49 721 608 7490; fax: +49 721 608 7492.
E-mail address: sekretariat@iwe.uni-karlsruhe.de (P. König).

0378-7753/$ – see front matter © 2008 Elsevier B.V. All rights reserved.
doi:10.1016/j.jpowsour.2008.07.045

Nomenclature

A	area (m^2)
c	species concentration ($mol\,m^{-3}$)
C_p	molar heat capacity ($J\,mol^{-1}\,K^{-1}$)
d	thickness (m)
D	diffusion coefficient ($m^2\,s^{-1}$)
$\Delta_r G$	Gibbs free reaction energy ($kJ\,mol^{-1}$)
$\Delta_r G^0$	Gibbs free reaction energy at standard pressure ($kJ\,mol^{-1}$)
$\Delta_r H$	reaction enthalpy ($kJ\,mol^{-1}$)
$\Delta_r \dot{H}$	reaction heat flow (W)
$\Delta \dot{H}_{VC}$	vaporisation, condensation reaction heat flow (W)
$\Delta_r S$	reaction entropy ($kJ\,mol^{-1}\,K^{-1}$)
E_{act}	activation energy (J, eV)
h	molar enthalpy ($J\,mol^{-1}$)
H	enthalpy (J)
$\dot{H}$	enthalpy flow (W)
I	current (A)
j	current density ($A\,cm^{-2}$)
j_0	exchange current density ($A\,cm^{-2}$)
j_{FC}	fuel cell current density ($A\,cm^{-2}$)
j_B	maximum boundary current density ($A\,cm^{-2}$)
k	heat transfer coefficient ($W\,m^{-2}\,K^{-1}$)
kA	area-averaged heat transfer coefficient ($W\,K^{-1}$)
K_p	equilibrium constant
n	molar amount (mol)
$\dot{n}$	molar flow ($mol\,s^{-1}$)
p^0	standard pressure (1.013 bar)
p_i	partial pressure of the component i (bar)
p^{sat}	saturation vapor pressure (bar)
$\dot{Q}$	heat flow (W)
R	ohmic resistance (Ω)
R	gas constant ($8.3145\,J\,mol^{-1}\,K^{-1}$)
S_{CO}	percentage CO selectivity (%)
T	temperature (K or °C)
T_0	temperature at standard conditions (298 K)
U_{CO}	percentage CO conversion (%)
U	voltage (V)
U_0	open circuit voltage (V)
U_{rev}	reversible cell voltage (V)
x	extend of reaction ($mol\,s^{-1}$)

Greek letters

α	heat conductivity coefficient ($W\,m^{-2}\,K^{-1}$)
δ	thickness (m)
η_{act}	activation overvoltage (V)
η_{diff}	diffusion overvoltage (V)
η_Ω	ohmic overvoltage (V)
λ	specific heat conduction capability ($W\,m^{-1}\,K^{-1}$)
ν	stoichiometric coefficient
ρ	specific resistance ($\Omega\,m$)

aided analysis environment has been developed. This tool is able to assist hardware test routines and – on the basis of the accessible data of a system with the help of a general system model – a method has been validated which enables an evaluation of the systems, helps recognise the efficiency of individual system components, reveals the problems during operation and allows an appraisal of the further optimisation potential of the systems.

As described earlier [1,2] the modelling is based on a general variable and flexible system model structure consisting of different subsystem groups. This structure provides a frame for all kinds of fuel cell systems (e.g. combined heat and power systems (CHP) or auxiliary power units (APU)) and was implemented in Matlab/Simulink™, creating a flexible modelling and simulation environment.

3.1. System model structure and topology

The main benefit of the presented model-aided analysis tool is its modularity and standardised build-up. Starting from the basis model structure the functional subgroups are split into further model levels according to the chosen top-down-strategy. The flexible model structure for components and the system allows the use of already existing and own developed models in nearly any grade of detail.

In Fig. 4 an example for a main subsystem group (fuel processing) is shown including the standard interface arrays, which are used in the subsystem groups and the models itself for a defined data exchange.

The main subsystem groups are then filled by connection of different component models matching the system setup. The fuel processing is thus able to represent the different fuel processing setups, e.g. for methane-based stationary PEMFC systems, methanol-based PEMFC APU or methane- and diesel-based stationary SOFC systems (Fig. 5).

3.2. Component model library and assumptions

For the different system components a model library was established (Fig. 6). This model library consists of steady state or dynamic electrical component models (blowers, compressors, pumps, inverters and other power electronic devices), general component models including a species and heat balance for steady state and dynamic simulation (reformer steps, heat exchanger, vaporisers and burners) and extended general models including electrochemistry for fuel cells. The component models provide standardised interfaces and allow a steady state and dynamic simulation of systems in any detail.

The standardised model structure as well as the C-Code compatibility of Matlab/Simulink™ provides an easy adaptation of literature models [7,8] or models in more detail [9] for simulation.

3.2.1. Chemical equilibrium calculation and species balance

For the chemical equilibrium calculation and the species balance ideal gases, incompressible liquids, total mixing and no pressure changes in the reaction volume are assumed.

For reversible chemical reactions the relation between the participating species and their stoichiometric coefficients ν is as follows [10,11]:

$$\nu_a A + \nu_b B \rightleftharpoons \nu_c C + \nu_d D \tag{1}$$

For a reaction in chemical equilibrium ($\Delta_r G = 0$) together with the definition for the equilibrium constant K_p it can be written:

$$\ln K_p = \frac{-\Delta_r G^0(T)}{RT} = \sum_i \left(\nu_i \ln \left(\frac{p_i}{p_i^0} \right) \right) \tag{2}$$

Eq. (1) together with the ideal gases law leads to Guldberg's law [10,12]:

$$K_p = \frac{\dot{n}(C)^{\nu_c} \dot{n}(D)^{\nu_d}}{\dot{n}(A)^{\nu_a} \dot{n}(B)^{\nu_b}} \frac{1}{(\dot{n}^0)^{(\nu_c+\nu_d-\nu_a-\nu_b)}} \tag{3}$$

The extend of reaction x describes the converted species amount per time of the reactions i. With the stoichiometric coefficients of the species taking part at the reactions and the conducted molar

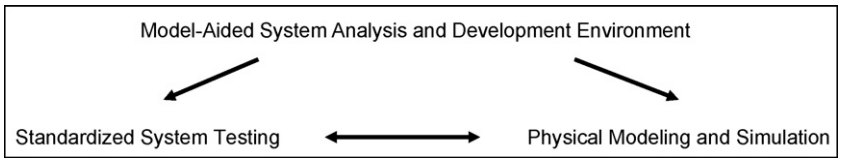

Fig. 1. Realised solution for an effective analysis and optimisation of fuel cell systems.

flows $\dot{n}_{\text{in}}$ a common equation system according to Eq. (3) can be established:

$$K_{p,i} = \exp\left(\frac{-\Delta_r G_i^0}{RT}\right) = \frac{(\dot{n}(C_i)_{\text{in}} + \nu_{c,i}x_i)^{\nu_{c,i}}(\dot{n}(D_i)_{\text{in}} + \nu_{d,i}x_i)^{\nu_{d,i}}}{(\dot{n}(A_i)_{\text{in}} + \nu_{a,i}x_i)^{\nu_{a,i}}(\dot{n}(B_i)_{\text{in}} + \nu_{b,i}x_i)^{\nu_{b,i}}} \frac{1}{(\dot{n}_i^0)^{(\nu_{c,i}+\nu_{d,i}-\nu_{a,i}-\nu_{b,i})}} \quad (4)$$

The resulting equilibrium molar flows of the products can then be written as

$$\begin{aligned} \dot{n}(A_i)_{\text{out}} &= \dot{n}(A_i)_{\text{in}} + \nu_{a,i}x_i \\ \dot{n}(B_i)_{\text{out}} &= \dot{n}(B_i)_{\text{in}} + \nu_{b,i}x_i \\ \dot{n}(C_i)_{\text{out}} &= \dot{n}(C_i)_{\text{in}} + \nu_{c,i}x_i \\ \dot{n}(D_i)_{\text{out}} &= \dot{n}(D_i)_{\text{in}} + \nu_{d,i}x_i \end{aligned} \quad (5)$$

The heat of the reaction flow $\Delta_r\dot{H}$ (exothermic or endothermic) can be calculated out of the sum of the reaction enthalpy weighted with extend of reactions:

$$\Delta_r\dot{H} = \sum_i x_i \Delta_r H_i \quad (6)$$

At appropriate pressure and temperature conditions vaporisation or condensation can occur in the reaction volumes. The resulting heat flow $\Delta\dot{H}_{\text{VC}}$ can be calculated with the enthalpy difference of the species i phase change from liquid (l) to gaseous (g) and vice versa:

$$\Delta\dot{H}_{\text{VC},i} = \Delta h_{\text{VC},i}\dot{n}_i^{\text{VC}} = (h_i^g - h_i^l)\dot{n}_i^{\text{VC}} \quad (7)$$

The enthalpy difference of the different species is approximated by temperature-dependant polynomials using according state diagrams [13,14]. For the enthalpy difference of water the following

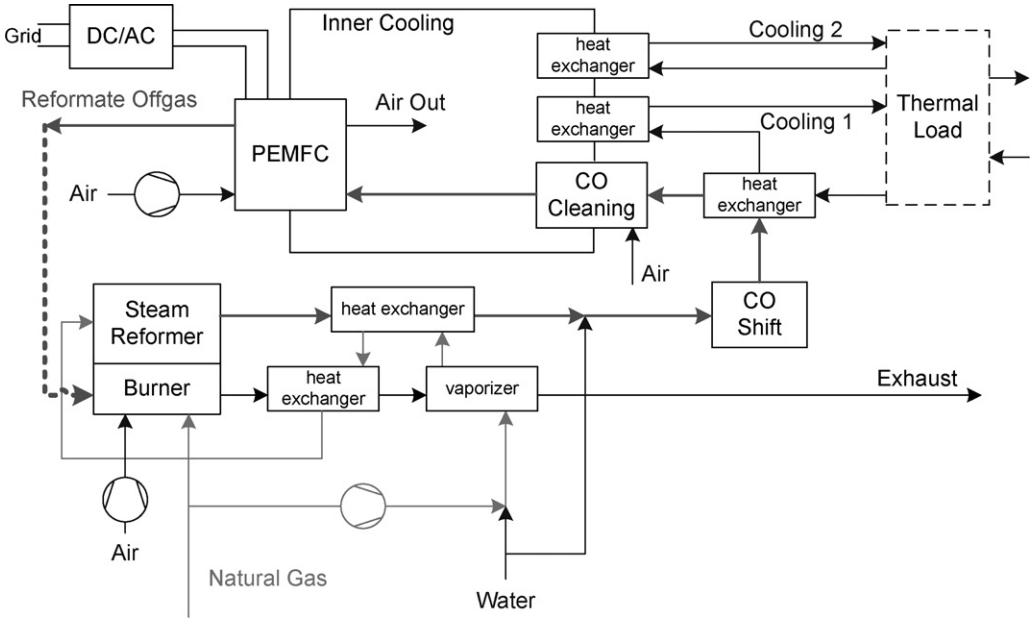

Fig. 2. System diagram of the stationary natural gas 2 kW_{el} PEMFC system *EDISon* at the IWE.

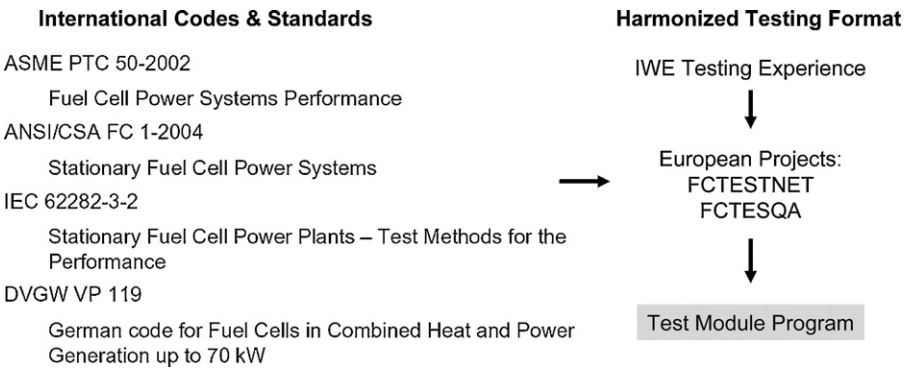

Fig. 3. Definition of standardised system test routines.

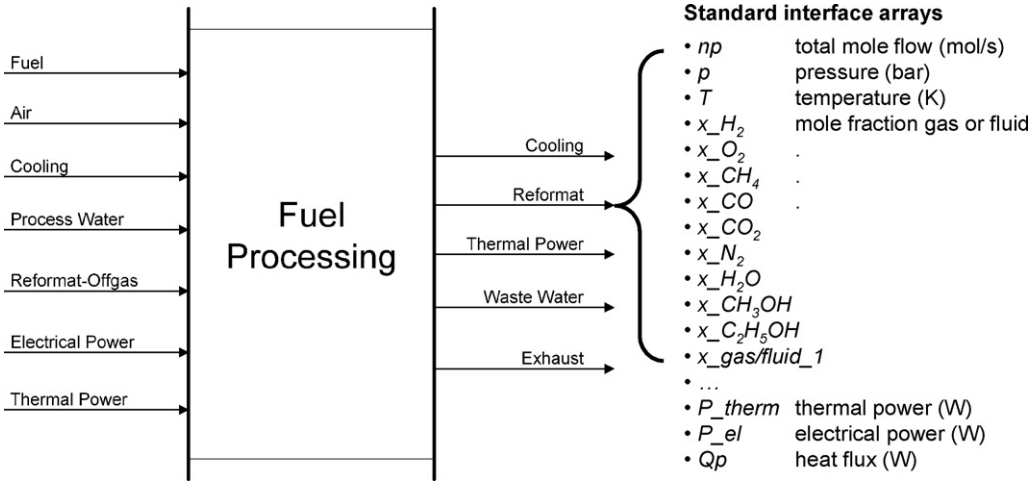

Fig. 4. Example of a main subsystem group including the composition of the standardised interface array.

polynomial is used (T in °C):

$$h^{g}_{H_2O} - h^{l}_{H_2O} = 45070 - 41.9T + 3.44 \times 10^{-3}T^2 + 2.54 \times 10^{-6}T^3 - 8.98 \times 10^{-10}T^4 \quad (\mathrm{J\,mol^{-1}}) \qquad (8)$$

The amount of the vaporising or condensing species $\dot{n}_i^{VC}$ is dependant on the steam mole flow $\dot{n}_i^{g}$ in the gas, the liquid phase $\dot{n}_i^{l}$ and the temperature-dependant saturation amount $\dot{n}_i^{sat}$. For the heat balance modelling a prefix-afflicted assignment is posted dependant on the saturation vapor pressure p_i^{sat} and the total pressure p_{tot}:

$$\dot{n}_i^{VC} = \begin{cases} \dot{n}_i^{g} - \dot{n}_i^{sat}, & \text{for } \{[(\dot{n}_i^{sat} \geq 0) \wedge (p_i^{sat} \leq p_{tot})] \wedge [(\dot{n}_i^{g} - \dot{n}_i^{sat}) > 0]\} \vee \{[(\dot{n}_i^{sat} \geq 0) \wedge (p_i^{sat} \leq p_{tot})] \wedge [(-\dot{n}_i^{l} \leq \dot{n}_i^{g} - \dot{n}_i^{sat}) \wedge (\dot{n}_i^{g} - \dot{n}_i^{sat} < 0)]\} \\ -\dot{n}_i^{l}, & \text{for } \{[(\dot{n}_i^{sat} \geq 0) \wedge (p_i^{sat} \leq p_{tot})] \wedge [(-\dot{n}_i^{l} > \dot{n}_i^{g} - \dot{n}_i^{sat}) \wedge (\dot{n}_i^{g} - \dot{n}_i^{sat} < 0)]\} \vee \{(p_i^{sat} > p_{tot})\} \\ 0, & \text{for } \{[(\dot{n}_i^{sat} \geq 0) \wedge (p_i^{sat} \leq p_{tot})] \wedge [(\dot{n}_i^{g} = 0) \wedge (\dot{n}_i^{l} = 0)]\} \end{cases} \qquad (9)$$

The steam saturation amount per time $\dot{n}_i^{sat}$ of a species in the gas flow can be calculated out of the ideal gases law and the partial pressures and molar flows of the different components. At constant pressure and temperature this leads to

$$\dot{n}_i^{sat} = \frac{p_i^{sat}}{p_{tot} - p_i^{sat}} \dot{n}_{tot,dry} \qquad (10)$$

3.2.2. Energy balance and heat transfer

For the energy balance and the heat transfer ideal gases, total mixing and incompressible liquids are assumed.

Volumes and masses of the system components are responsible for the dynamic of the heat transfer influencing the thermal behaviour of the components. Regarding energy and mass conservation for any open system a dynamic energy balance can be posted, which includes the conducted and dissipated heat and enthalpy flows of the system:

$$\frac{dH}{dt} = \dot{Q}_{in} - \dot{Q}_{out} + \dot{H}_{in} - \dot{H}_{out} \qquad (11)$$

According to [10] the enthalpy H of ideal gases is

$$H = nh = nC_p(T - T^0_{298\,K}) \qquad (12)$$

Together with Eq. (11) this leads to

$$\frac{dH}{dt} = \sum_i n_i C_{p,i} \frac{dT}{dt} = \dot{Q}_{in} - \dot{Q}_{out} + \dot{H}_{in} - \dot{H}_{out} \qquad (13)$$

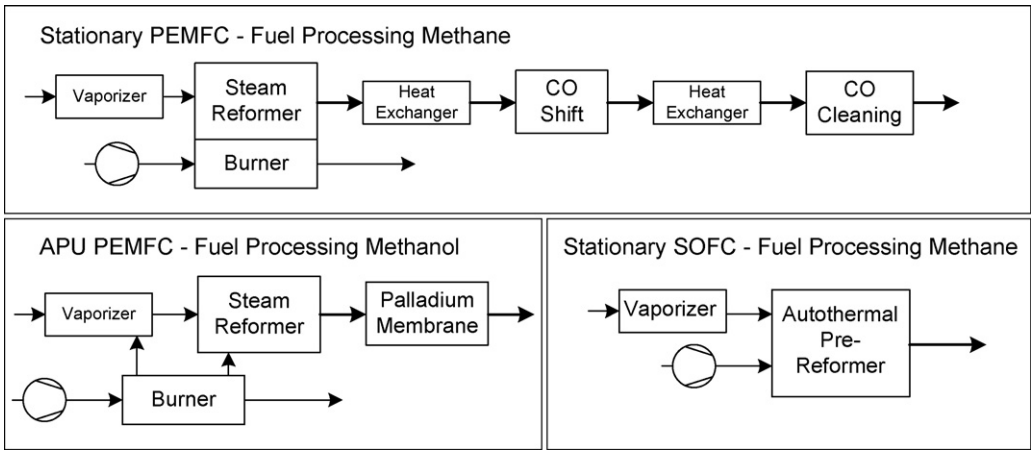

Fig. 5. Different types of fuel processing setups represented by the main subsystem group fuel processing.

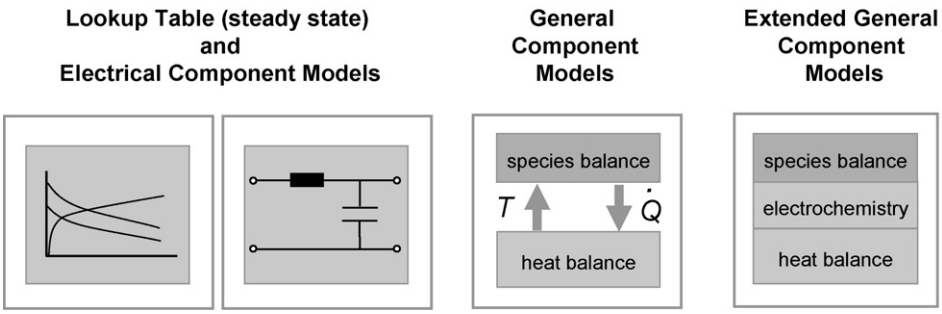

Fig. 6. Structure of the component model library providing standardised interfaces for steady state and dynamic simulations of systems.

$\dot{H}_{\text{in}}$ and $\dot{H}_{\text{out}}$ represent the sum of all conducted and dissipated molar enthalpy flows [10]:

$$\dot{H}_{\text{in}} = \sum_{i=1}^{n} \dot{H}_{i,\text{in}} = \sum_{i=1}^{n} \dot{n}_i C_{p,i}(T - T^0_{298\,\text{K}})$$
$$\dot{H}_{\text{out}} = \sum_{i=1}^{m} \dot{H}_{i,\text{out}} = \sum_{i=1}^{m} \dot{n}_i C_{p,i}(T - T^0_{298\,\text{K}}) \quad (14)$$

Accordingly for the heat flows $\dot{Q}_{\text{in}}$ and $\dot{Q}_{\text{out}}$:

$$\dot{Q}_{\text{in}} = \sum_{i=1}^{n} \dot{Q}_{i,\text{in}}$$
$$\dot{Q}_{\text{out}} = \sum_{i=1}^{m} \dot{Q}_{i,\text{out}} \quad (15)$$

For the heat conduction through a thin barrier the heat flow is dependant on heat conduction capability λ of the material, the thickness d of the barrier, the passed through barrier area A and the temperature difference ΔT between outside and inside the barrier:

$$\dot{Q} = \frac{\lambda}{\text{d}} A\,\Delta T \quad (16)$$

In case of convection a gas or a liquid is streaming along on side of the barrier absorbing heat and dissipating it at a different place. Analogue to Eq. (16) the heat flow is calculated using heat conductivity coefficient α:

$$\dot{Q} = \alpha A\,\Delta T \quad (17)$$

For the total heat transfer through a barrier, where two fluids (fluid 1 and fluid 2) are streaming along (e.g. a heat exchanger), the convection on both sides as well as the heat flow through the barrier has to be considered. Therefore a heat transfer coefficient k is calculated [15]:

$$\frac{1}{k} = \frac{1}{\alpha_1} + \frac{\text{d}}{\lambda} + \frac{1}{\alpha_2} \quad (18)$$

This leads to the heat flow transferred from volume 1 to volume 2:

$$\dot{Q} = kA\,\Delta T \quad (19)$$

The heat transfer coefficient and the temperature difference are only valid locally. Therefore area-averaged heat transfer coefficients (kA-values) and averaged temperature differences (ΔT) are used for calculation.

4. Stationary PEMFC CHP system process model and component assumptions

The extensive tested and analysed stationary PEMFC CHP system *EDISon* [1–3] (Fig. 2) operates on natural gas, which is converted to hydrogen by a steam reforming unit including a CO shift step. A CO purification is carried out by selective oxidation. The product gas, which is fed to the stack, exhibits a CO concentration <30 ppm. The PEMFC stack consists of 80 cells with an electrode area of 126 cm^2 each. Further components in the system are a methane burner, a desulphurisation unit, a water purifying unit, compressors for air and fuel and a power inverter for grid connection. The system shall supply max. 1.8 kW electricity and approximately 4 kW heating power for domestic hot water and space heating.

The system was used for performing specific simulation studies regarding hardware and efficiency optimisation. In the following chapters the main system components model assumptions are mentioned.

4.1. Methane steam reformer model assumptions

Together with the steam reforming reaction of methane the side reaction of the CO-shift occurs:

$$\begin{aligned}&(1)\ \text{CH}_4 + \text{H}_2\text{O} \rightleftharpoons \text{CO} + 3\text{H}_2 \quad \Delta_\text{r}H^0_{298K} = 206.1\,\text{kJ mol}^{-1}\\ &(2)\ \text{CO} + \text{H}_2\text{O} \rightleftharpoons \text{CO}_2 + \text{H}_2 \quad \Delta_\text{r}H^0_{298K} = -41.2\,\text{kJ mol}^{-1}\end{aligned} \quad (20)$$

This leads together with Eq. (4) to the reaction equation system:

$$K_{\text{p},1} = \exp\left(\frac{-\Delta_\text{r}G^0_1}{RT}\right) = \frac{(\dot{n}_{\text{CO,in}} + x_1 - x_2)(\dot{n}_{\text{H}_2,\text{in}} + 3x_1 + x_2)^3}{(\dot{n}_{\text{CH}_4,\text{in}} - x_1)(\dot{n}_{\text{H}_2\text{O,in}} - x_1 - x_2)} \times \frac{1}{(\dot{n}_{\text{tot,in}})^2} \quad \pm(21)$$
$$K_{\text{p},2} = \exp\left(\frac{-\Delta_\text{r}G^0_2}{RT}\right) = \frac{(\dot{n}_{\text{CO}_2,\text{in}} + x_2)(\dot{n}_{\text{H}_2,\text{in}} + 3x_1 + x_2)}{(\dot{n}_{\text{CO,in}} + x_1 - x_2)(\dot{n}_{\text{H}_2\text{O,in}} - x_1 - x_2)}$$

The resulting equilibrium molar flows of the product gas can be calculated out of Eq. (5) to

$$\begin{aligned}\dot{n}_{\text{H}_2,\text{out}} &= \dot{n}_{\text{H}_2,\text{in}} + 3x_1 + x_2\\ \dot{n}_{\text{CO,out}} &= \dot{n}_{\text{CO,in}} + x_1 - x_2\\ \dot{n}_{\text{CO}_2,\text{out}} &= \dot{n}_{\text{CO}_2,\text{in}} + x_2\\ \dot{n}_{\text{CH}_4,\text{out}} &= \dot{n}_{\text{CH}_4,\text{in}} - x_1\\ \dot{n}_{\text{H}_2\text{O,out}} &= \dot{n}_{\text{H}_2\text{O,in}} - x_1 - x_2\end{aligned} \quad (22)$$

The simulation parameters (reaction volumes and heat transfer coefficients) for the further component models of the reforming unit (steam reformer, burner, vaporiser and heat exchanger) are listed in Table 1.

4.2. CO-shift model assumptions

The model for the medium temperature shift (MTS) consists of the reaction equation for the CO shift:

$$\text{CO} + \text{H}_2\text{O} \rightleftharpoons \text{CO}_2 + \text{H}_2 \quad \Delta_\text{r}H^0_{298\,\text{K}} = -41.2\,\text{kJ mol}^{-1} \quad (23)$$

Table 1
EDISon CHP reaction volumes and heat transfer coefficients—reforming unit

Component	Volume primary (m^3)	kA-value primary ($W K^{-1}$)	Volume secondary (m^3)	kA-value secondary ($W K^{-1}$)	Mass solid (kg)	kA-value solid ($W K^{-1}$)
Methane steam reformer	4.37e−3	7	–	–	6	0.19
Methane burner	3.69e−3	0.1294	–	–	3	0
Vaporiser	9.13e−4	2.19	1e−4	3.1	0.703	1.2
Heat exchanger	2.54e−3	1.2	1.3e−4	2.5	0.824	0.3
Exhaust heat exchanger	1.81e−4	2.7	6.41e−3	6.3	1.144	1.512

The resulting equilibrium molar flows of the product gas are

$$\begin{aligned}\dot{n}_{H_2,out} &= \dot{n}_{H_2,in} + x\\ \dot{n}_{CO,out} &= \dot{n}_{CO,in} - x\\ \dot{n}_{CO_2,out} &= \dot{n}_{CO_2,in} + x\\ \dot{n}_{H_2O,out} &= \dot{n}_{H_2O,in} - x\end{aligned} \tag{24}$$

The simulation parameters (reaction volumes and heat transfer coefficients) for the further component models of the CO-shift unit (vaporiser, CO-shift and heat exchanger) are listed in Table 2.

4.3. CO purification model assumptions

For the CO purification using a selective methanation (SelMet) the model for the methane steam reforming can be used as reverse reaction.

For the CO purification using a selective oxidation (SelOx) aside the CO oxidation the H_2 oxidation occurs in parallel:

$$\begin{aligned}&(1)\ CO + \frac{1}{2}O_2 \rightleftharpoons CO_2 \quad \Delta_r H^0_{298\,K} = -282.9\,kJ\,mol^{-1}\\ &(2)\ H_2 + \frac{1}{2}O_2 \rightleftharpoons H_2O \quad \Delta_r H^0_{298\,K} = -241.8\,kJ\,mol^{-1}\end{aligned} \tag{25}$$

Setting a percentage CO conversion U_{CO} and a percentage CO selectivity S_{CO} the model can be adapted to different real reformers and measurement values:

$$\begin{aligned}U_{CO} &= \frac{\dot{n}_{CO,utilised}}{\dot{n}_{CO,in}}\\ S_{CO} &= \frac{\dot{n}_{O_2,CO-oxidation}}{\dot{n}_{O_2,utilised}}\end{aligned} \tag{26}$$

The resulting equilibrium molar flows of the product gas then are

$$\begin{aligned}\dot{n}_{H_2,out} &= \dot{n}_{H_2,in} - 2[\dot{n}_{O_2,in} - \dot{n}_{O_2,out} - 0.5(\dot{n}_{CO,in} - \dot{n}_{CO,out})]\\ \dot{n}_{CO,out} &= \dot{n}_{CO,in} - \frac{U_{CO}}{100}\dot{n}_{CO,in}\\ \dot{n}_{CO_2,out} &= \dot{n}_{CO_2,in} + (\dot{n}_{CO,in} - \dot{n}_{CO,out})\\ \dot{n}_{H_2O,out} &= \dot{n}_{H_2O,in} + 2[\dot{n}_{O_2,in} - \dot{n}_{O_2,out} - 0.5(\dot{n}_{CO,in} - \dot{n}_{CO,out})]\\ \dot{n}_{O_2,out} &= \dot{n}_{O_2,in} - \frac{(\dot{n}_{CO,in} - \dot{n}_{CO,out})100}{2S_{CO}}\end{aligned} \tag{27}$$

The simulation parameters (reaction volumes and heat transfer coefficients) for the further component models of the CO cleaning unit (SelOx and heat exchanger) are listed in Table 3.

4.4. PEMFC stack model assumptions

For the fuel cell model ideal gases, constant pressures along the channels, electrolyte only proton conductive and no further fluid transport are assumed.

The reaction equation for the H_2-oxidation is

$$H_2 + \frac{1}{2}O_2 \rightleftharpoons H_2O \quad \Delta_r H^{liquid}_{298\ K} = -285.8\,kJ\,mol^{-1} \tag{28}$$

The hydrogen requirement $\dot{n}_{H_2,req}$ of the fuel cell can be calculated depending on load current and number of cells using Faraday's law [16]:

$$\dot{n}_{H_2,req} = \frac{N}{zF}I_{load} = \frac{NA_{cell}}{zF}j_{FC} \tag{29}$$

The output molar flow composition of the anode and the cathode are calculated using Eq. (28) and the chemical equilibrium

Table 2
EDISon CHP reaction volumes and heat transfer coefficients—CO-shift unit

Component	Volume primary (m^3)	kA-value primary ($W K^{-1}$)	Volume secondary (m^3)	kA-value secondary ($W K^{-1}$)	Mass solid (kg)	kA-value solid ($W K^{-1}$)
Vaporiser	0.05	–	–	–	–	–
CO-shift	0.88e−6	1.25	–	–	0.5	0.12
Heat exchanger	0.52e−3	6.5	0.52e−3	19	1e−5	6

Table 3
EDISon CHP reaction volumes and heat transfer coefficients—CO cleaning unit

Component	Volume primary (m^3)	kA-value primary ($W K^{-1}$)	Volume secondary (m^3)	kA-value secondary($W K^{-1}$)	Mass solid (kg)	kA-value solid ($W K^{-1}$)
Gas to gas heat exchanger	1.32e−3	2	5.21e−3	2	1e−5	2
Gas to liquid heat exchanger	3.77e−6	3	3.39e−3	2.8	0.15	0.01
SelOx	1e−5	14	–	–	1e−5	1

calculation regarding vaporisation and condensation:

$$\begin{aligned}\dot{n}_{H_2,A,out} &= \dot{n}_{H_2,A,in} - \dot{n}_{H_2,req}\\ \dot{n}^{g}_{H_2O,A,out} &= \dot{n}^{g}_{H_2O,A,in} - \dot{n}^{VC}_{H_2O,A}\\ \dot{n}_{O_2,C,out} &= \dot{n}_{O_2,C,in} - \frac{1}{2}\dot{n}_{H_2,req}\\ \dot{n}^{g}_{H_2O,C,out} &= \dot{n}^{g}_{H_2O,C,in} + \dot{n}_{H_2,req} - \dot{n}^{VC}_{H_2O,C}\end{aligned} \tag{30}$$

The cell voltage is assumed to be

$$U_{cell} = U_{rev} - \eta_{act} - \eta_{diff} - \eta_{\Omega} \tag{31}$$

The temperature and pressure dependant reversible cell voltage for the hydrogen oxidation can be written as [10,16–19]:

$$U_{rev} = \frac{-\Delta_r G^0}{zF} + \frac{\Delta_r S}{zF}(T - T_0) + \frac{RT}{zF}\ln\left(\frac{p_{H_2}\sqrt{p_{O_2}}}{p_{H_2O}\sqrt{p^0}}\right) \tag{32}$$

The exchange current density j_0 is temperature and concentration dependant [16,17]. In [19] the exchange current density is described dependant on the concentrations C_{ox} and C_{red}, the activation energy E_{act}, the temperature T and a so-called frequency factor $\bar{A}$:

$$j_0 = zF\bar{A}c_{ox}^{1-\alpha}c_{red}^{\alpha}\,e^{-E_{act}/kT} \tag{33}$$

In the model the activation overvoltage η_{act} is calculated regarding an anode and cathode part for the exchange current density in Eq. (33). Assuming constant concentrations at anode and cathode, these concentrations lead together with the frequency factor to a new factor A. The activation energy E_{act} and the Boltzmann constant are combined to a factor B. In case of ideal gases the concentrations can be replaced by partial pressures p_i. This leads to the expressions for the exchange current densities at the anode $j_{0,A}$ and at the cathode $j_{0,C}$:

$$\begin{aligned}j_{0,A} &= A_A p_{H_2}^{(1-\alpha_A)}\frac{zF}{RT_A}e^{-B_A/T_A}\\ j_{0,C} &= A_C p_{O_2}^{\alpha_C}\frac{zF}{RT_C}e^{-B_C/T_C}\end{aligned} \tag{34}$$

For the modelling of the diffusion a simplified one-dimensional system assuming a linear concentration decrease through the electrode is used [16,19]. Together with the first Fick's law it can be written as

$$j_{FC} = \frac{I_{FC}}{A_{cell}} = zFD_i\frac{c_i - c_{PB,i}}{\delta_i} \tag{35}$$

The current limit is reached, when the boundary phase reaction is faster than the charge carrier diffusion through the electrodes and thus reaching a zero phase boundary concentration $c_{PB,i}$. This leads to the maximum boundary current density $j_{B,max}$ using the ideal gases law:

$$j_{B,max} = zFD_i\frac{c_i}{\delta_i} = zFD_i\frac{p_i}{RT\delta_i} \tag{36}$$

At the boundary between gas volume and electrode the potential U is [19]:

$$U = U_0 - \frac{RT}{zF}\ln\frac{c_i}{c_i^0} \tag{37}$$

At the phase boundary:

$$U_{PB,i} = U_0 - \frac{RT}{zF}\ln\frac{c_{PB,i}}{c_i^0} \tag{38}$$

Table 4
PEMFC stack voltage current curve model parameters

Open circuit voltage	U_0	0.95 V
Fuel utilisation anode	–	90%
Air utilisation cathode	–	30%
Exchange current density anode	$j_{0,A}$	280 mA cm^{-2}
Exchange current density cathode	$j_{0,K}$	1.8 mA cm^{-2}
Transfer factor anode	α_A	0.4
Transfer factor cathode	α_K	0.72
Specific resistance anode	ρ_A	1.4e−3 Ω cm
Specific resistance membrane	ρ_M	25 Ω cm
Specific resistance cathode	ρ_K	1.2e−3 Ω cm
Thickness anode	δ_A	100 μm
Thickness membrane	δ_M	175 μm
Thickness cathode	δ_K	100 μm
Diffusion coefficient anode	D_A	1e−7 m^2 s^{-1}
Diffusion coefficient cathode	D_K	9e−8 m^2 s^{-1}
Factor anode	B_A	0
Factor cathode	B_K	1/5000

Table 5
EDISon CHP reaction volumes and heat transfer coefficients—PEMFC stack unit

kA-value anode	7 W K^{-1}
kA-value cathode	7 W K^{-1}
kA-value cooling	50 W K^{-1}
kA-value solid	0.5 W K^{-1}
Mass solid	12 kg
Volume cooling	0.5 l
Channel size anode	0.5 mm
Channel size cathode	0.5 mm

The difference of the electrochemical potentials within the electrodes, caused by the species transport, leads to the diffusion overvoltage η_{diff}:

$$\begin{aligned}\eta_{diff} &= U - U_{PB,i} = \frac{RT}{zF}\ln\frac{c_{PB,i}}{c_i}\\ &= \frac{RT}{zF}\ln\left(1 - \frac{j_{FC}\delta_i}{zFD_ic_i}\right) = \frac{RT}{zF}\ln\left(1 - \frac{j_{FC}}{j_{B,max}}\right)\end{aligned} \tag{39}$$

For the Ohmic overvoltage η_{Ω} a linear increase with the current density is assumed. Therefore constant specific resistances ρ_i for the electrodes and for the membrane can be implied:

$$\eta_{\Omega} = RI_{FC} = (\rho_A\delta_A + \rho_M\delta_M + \rho_C\delta_C)j_{FC} \tag{40}$$

The stack voltage current curve model parameters used in the simulations are displayed in Table 4.

Additional simulation parameters (geometry, reaction volumes and heat transfer coefficients) for the PEMFC stack unit are listed in Table 5.

Table 6
EDISon CHP steady state operating points, coolant 25 °C, fuel utilisation 50%

System operating point	50%	60%	70%
Conducted methane heating power (kW)	6.65	8.41	8.5
Produced H2 power (kW)	3.7	4.4	5.15
Electrical power (kW)	0.935	1.09	1.15
Thermal power (kW)	1.5	1.9	2.15
Electrical efficiency (%)	14.06	12.96	13.53
Electrical net efficiency (%)	8.05	8.2	8.82
Thermal efficiency (%)	22.6	22.59	25.3
Total net efficiency (%)	30.65	30.79	34.12
Total efficiency (%)	36.66	35.55	38.83

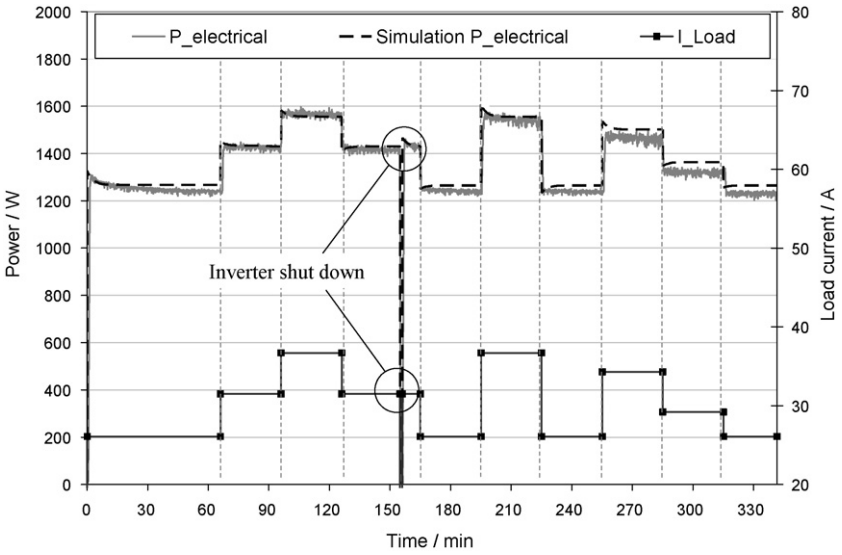

Fig. 7. Response dynamics for measured and simulated electrical system power output.

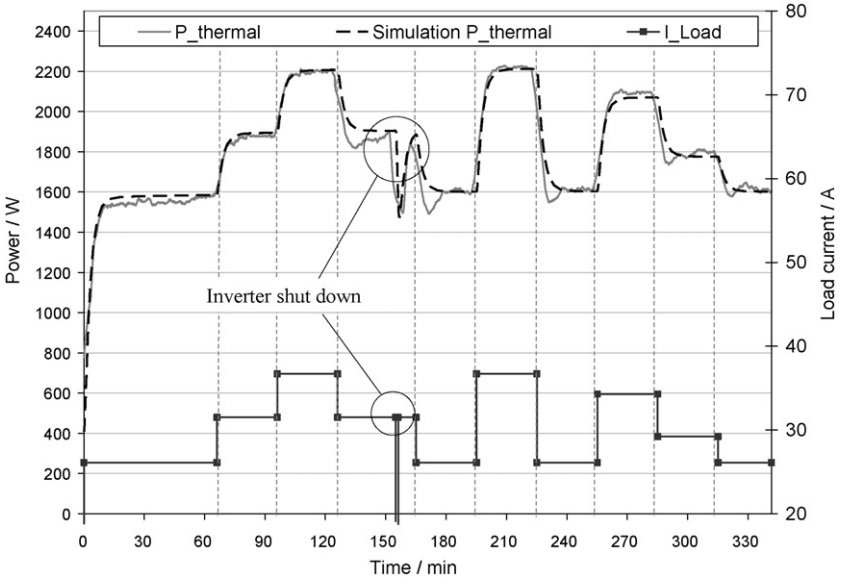

Fig. 8. Response dynamics for measured and simulated thermal system power output.

5. Results and discussion

The measurement results of the 1.8 kW_{el} and 4 $kW_{thermal}$ PEMFC CHP prototype system *EDISon* showed a limited possible system operating range of 50–70% maximum electrical output power due to the system configuration and control. The suboptimal cathode flow duct concept of the PEMFC stack leads to a maximum possible fuel utilisation of only 50% over the system operating range. In Table 6 the reached steady state system operating points at 25 °C coolant temperature and at a fuel utilisation of 50% are displayed.

Using the developed physical models for the different reformer steps, PEMFC, heat exchangers and compressors a system model was built to simulate the different testing procedures performed prior to the simulation. In Figs. 7 and 8 a measured typical standardised dynamic test module is shown. During the measurement the system output power is varied by changing the load current including an inverter shutdown. The simulation results show a good agreement with the measured electrical and thermal power outputs. Even the electrical load step response dynamics of the PEMFC stack power output can be simulated with a good accuracy (Fig. 7).

Based on the measurement results the former validated model-aided system analysis environment is now used to detect the optimisation potential of the prototype PEMFC CHP system and to show the available real performance values of the system and its components.

The identified main criteria resulting in poor system performance are: power loss due to falsely designed and faulty components, efficiency loss due to parasitic auxiliaries, efficiency loss due to ineffective component setup and system technology, poor system insulation and heat integration as well as inappropriate concepts for fuel treatment and fuel cell operation. All these points are directly influencing the efficiency and therefore the performance of the systems. Aside the economical optimisation and the long-term stability the increase of the efficiency therefore represents a main development demand for stationary fuel cell systems.

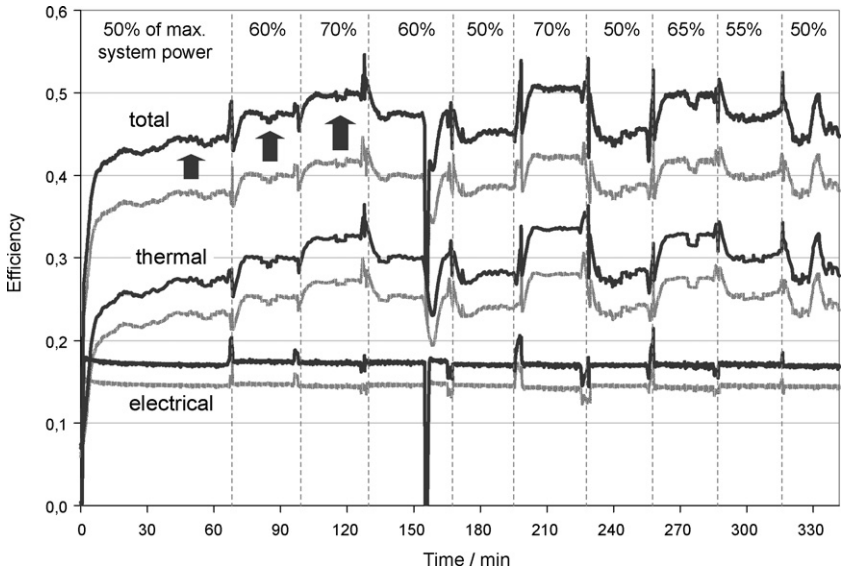

Fig. 9. Simulation results: thermal, electrical and total efficiency of the stationary natural gas 2 kW_{el} PEMFC system without (light colour) and with (dark colour) anode offgas recirculation to the burner.

5.1. Increase of the fuel utilisation

The measurement results and the performed post-test simulation analyses on the PEMFC CHP system showed, that for a as high as possible efficiency the fuel stack as the central energy converter has to be designed and operated as optimal as possible. Especially during reformate gas operation the maximum achievable fuel utilisation in the fuel cell stack has an essential influence on system performance and efficiency.

The maximum achievable system efficiencies at varying fuel utilisation are listed in Table 7. By increasing the fuel utilisation from 50% to an aiming realistic value of 80%, absolute efficiency increases of 5.4% electrical and 11.5% thermal have been determined for the analysed system. This can be achieved by optimising the flow duct in the stack and reducing the inert gases in the reformat gas flow.

5.2. Reduced electric auxiliaries consumption

In every steady state operating point the analysed system has an electrical power consumption due to the auxiliaries of about 400 W. In relation to the produced power there is a high potential for efficiency optimisation. In Table 8 the achievable system efficiencies at a fuel utilisation of 70% and an averaged auxiliaries power consumption of 400 W are displayed. By reducing the power consumption down to 100 W an electrical net efficiency increase up to 3.5% can be achieved.

Table 7
EDISon CHP efficiencies, variation of fuel utilisation, coolant 25 °C, power setpoint 70%

Fuel utilisation anode	50%	70%	80%
Electrical efficiency (%)	12.99	16.84	18.37
Electrical net efficiency (%)	7.65	11.51	13.04
Thermal efficiency (%)	21.17	29.21	32.65
Total efficiency (%)	34.16	46.05	51.02
Total net efficiency (%)	28.82	40.72	45.69

Table 8
EDISon CHP variation of electric losses, coolant 25 °C, power setpoint 70%

Electrical auxiliaries losses	400 W	200 W	100 W
Conducted methane heating power (kW)	8.5	8.5	8.5
Electrical power (kW)	1.431	1.431	1.431
Electrical efficiency (%)	16.84	16.84	16.84
Electrical net efficiency (%)	12.13	14.48	15.66

5.3. Reduced primary energy consumption—feeding back of the anode offgas

Analysing the performed system measurements and simulations [1,2] it was possible to quantify the feasible efficiency increase of the methane-based stationary PEMFC CHP system when feeding back the anode offgas to the burner (Fig. 2) and therefore saving methane. In Fig. 9 the simulation results predict an average absolute efficiency increase of 5% electrical and 3% thermal.

5.4. Reduced primary energy consumption—increase of the reformer heat insulation

Using an infrared camera the radiated heat losses of the PEMFC CHP system reformer unit have been visualised. At the specific system operating point (50% system power) a reformer outlet temperature of 803.4 °C and a methane consumption in the burner of 4.604×10^{-3} mol s^{-1} have been measured. The average heat trans-

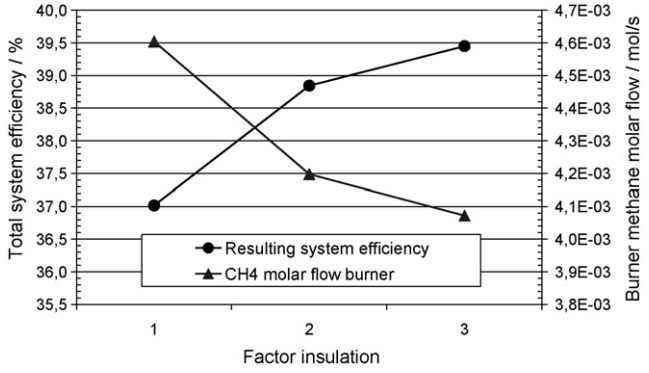

Fig. 10. Simulated possible methane consumption reduction of the burner by increasing the insulation as well as the resulting increase of the total system efficiency at 50% system power.

Table 9
EDISon CHP simulated gas composition after the CO-shift step

Parameter		Gas composition	
Educt H_2O	0.02976 mol s^{-1}	H_2 (vol.%)	79.43
Educt CH_4	0.00473 mol s^{-1}	CO (vol.%)	0.3063
Educt N_2	0.00116 mol s^{-1}	CO_2 (vol.%)	19.63
Pressure	1.04 bar(a)	CH_4 (vol.%)	0.1255
Temperature reformer	806.9 °C	N_2 (vol.%)	0.5143
Temperature CO shift	275.6 °C		

Table 11
EDISon CHP system types 1 and 2, determined maximum system efficiencies

System type	SelOx	SelMet
Electrical efficiency (%)	16.84	17.01
Electrical net efficiency (%)	11.51	11.67
Thermal efficiency (%)	29.21	28.95
Total efficiency (%)	46.05	45.96
Total net efficiency (%)	40.72	40.62

fer coefficient (kA-value) from the reformer solid mass to the environment has then been determined by simulation.

The model was then parameterised with these values. With simulation studies the possible decrease of the heat losses by increasing the reformer insulation was determined. Fig. 10 shows the reduction of the natural gas molar flow depending on the insulation as well as the resulting total system efficiency. By increasing the insulation the necessary natural gas molar flow is reduced. The amount for the reforming is kept constant. Using a three times larger insulation (kA-value: 0.063 W K^{-1}) the necessary natural gas amount would be reduced by 11.6%. This would then result in an absolute system efficiency increase (excluding auxiliaries losses) of 2.45%.

5.5. Optimised concept for the fuel treatment

An essential advantage of the developed modelling and simulation approach is the possible simulation of different kinds of system configurations by easily replacing components in the model.

A very promising point in system optimisation is to rearrange or to exchange system components to improve the thermal integration or to reduce parasitic components and to simplify the system technology. The present natural gas reformer unit of our stationary PEMFC system consists of a subunit including a steam reformer step (STR) and a CO cleaning step (MTS). The needed CO fine cleaning step (selective oxidation) is installed separately including the needed additional air dosing increasing the auxiliary losses.

To be able to remove the necessary air dosing and compressed air supply, in our model the SelOx has been replaced with a selective methanation step (SelMet) (Fig. 11).

Additionally a better thermal integration can be achieved by a direct mounting of the SelMet into the reformer unit. The exothermic reaction of the SelMet, as reverse reaction of the methane steam reformation, allows an optimised thermal management and therefore saving reformer unit heating power.

The main important aspect was to guarantee that the gas quality of the resulting reformation was equal or even better than before. Performed simulation studies were able to proof the concept. In Table 9 the selected model parameters of the steam reformer and the CO shift as well as the resulting output gas composition of the CO shift at 60% system power are displayed.

In Table 10 the according resulting product gas compositions for the SelOx and SelMet at the 60% system operating point are listed.

For the SelMet the simulation shows a higher hydrogen amount of 79.22% in the product gas and nearly no CO compared to the SelOx. Due to the different chemical reactions the SelMet shows a lower methane conversion rate. In comparison to the reduced

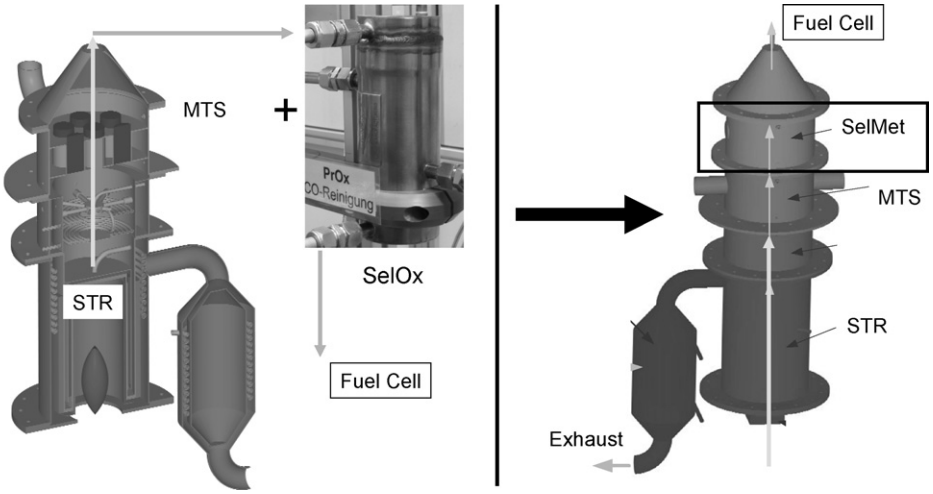

Fig. 11. (Left) CO fine cleaning by selective oxidation unit (SelOx). (Right) Replacement by selective methanation (SelMet).

Table 10
EDISon CHP gas quality comparison SelOx and SelMet, power setpoint 60%

Parameter	SelOx	SelMet	Gas composition	SelOx	SelMet
Temperature	45 °C	246.85 °C	H_2 (vol.%)	75.09	79.22
Pressure	1.04 bar(a)	1.04 bar(a)	CO (ppm)	5.33	2.364×10^{-5}
Educt O_2	0.00148 mol s^{-1}	–	CO_2 (vol.%)	19.28	19.5
Utilisation CO	99.82%	–	CH_4 (vol.%)	0.1214	0.7439
Utilisation CO_2	–	1.5%	N_2 (vol.%)	5.248	0.5269
CO selectivity	14.5%	–	O_2 (vol.%)	0.2591	–
			CH_4 conversion (%)	99.4	96.38

Table 12
Optimised EDISon CHP system type 2 compared to pre-commercial systems

System	Prototype EDISon 2 (optimised min. values)	Viessmann Lab type 2 [20,21]	Viessmann Lab type 3 [20,21]	Vaillant EURO 2 [20,22]
Fuel	Natural gas	Natural gas	Natural gas	Natural gas
Electrical power	1.5 kW	2 kW	2 kW	4.5 kW
Electrical net efficiency (%)	21.73	23	28	>35 (target)
Thermal efficiency (%)	35.39	44	48	>45 (target)
Total net efficiency (%)	59.57 (57.12)	67	76	>80 (target)

system components (no additional air input) and the optimised CO reduction yet this is negligible.

The small amount of nitrogen in the product gas of the SelMet is a result of the conducted natural gas composition. This obvious minimised inert amount of nitrogen in the conducted reformate gas flow of the SelMet in comparison to the SelOx reduces the occurring species transport blockings at high load currents in the PEMFC stack and therefore better hydrogen conversion rates are possible.

The absence of the SelOx in the coolant circuit of the fuel cell stack unit also allows higher stack operating temperatures and therefore higher power levels due to the missing limited SelOx operating temperature of 45 °C.

The benefit of the possible efficiency increase is only then valid, if already at the same operating conditions (coolant temperature, fuel utilisation, load current) as with the SelMet similar output power levels are reached. The simulation results of the power output comparison of the different system configurations with SelOx (EDISon CHP system type 1) and SelMet (EDISon CHP system type 2) are displayed in Table 11.

The SelMet system achieves a higher electrical efficiency of 0.17% absolute. The SelOx system has therefore a 0.26% absolute higher thermal efficiency. The total efficiencies of both systems are therefore almost identical and the above-mentioned advantages of the EDISon CHP system type 2, better thermal integration and absence of the air supply, allow an effective system efficiency increase.

5.6. *Efficiency optimised simulated system compared to real pre-commercial systems*

Out of the sum of the above-mentioned possible efficiency increases, determined with the standardised test procedures and the modelling and simulation approach, a minimum value prediction for the achievable system efficiencies can be stated and compared to existing systems (Table 12).

Therefore the EDISon CHP system type 2 (SelMet) serves as an optimisation basis regarding the efficiency increase using anode recirculation and optimised reformer insulation. Additionally the possible absolute efficiency increases achieved with a fuel utilisation increase from 70% to 80% (simulated values: 1.53% electrical, 3.44% thermal) as well with a reduction of the auxiliaries electrical consumption to 100 W (3.53% net electrical, Table 8) are considered.

Comparing the predicted values of the EDISon 2 system with the data of the almost similar concept of the industrial Viessmann lab prototype 2 [20,21] the applicability and ability for realistic and exact predictions of the developed model-aided analysis and simulation approach can be proven.

Having a still optimised reformer concept the Viessmann lab prototype achieves a better total system efficiency. With the additional improvements by a more compact reformer concept, lower reformer temperatures and the resulting reduction of primary energy similar to the Viessmann lab prototype 3 [20,21] the EDISon 2 system could achieve comparable electrical system efficiencies of about 30%.

6. Conclusions

A model-aided system analysis and optimisation environment based on Matlab/Simulink™ has been developed and validated for different kinds of fuel cell systems. The approach of the standardised modelling and simulation environment including the likewise developed standardised system testing procedures [5,6] provides additional information about input and output values, internal variables of state as well as the system efficiency in the steady state and in the dynamic operation mode and thus proves itself a powerful tool.

The knowledge of the power and operating limits of the fuel cell systems leads to the development of optimisation strategies and the determination of the realisable system and component potential. In this work the most important points for the judgement of the system and component power and optimisation potential have been analysed:

- efficiency, modulation ability and system operating range;
- application evaluation of alternative or additional system components;
- optimisation of the thermal integration and reduction of thermal losses;
- hardware optimisation: system setup, reduce of parasitic system components.

Aside the economical optimisation and the long-term stability the increase of the system efficiency represents the main development demand for stationary fuel cell systems. Using the developed modelling and simulation approach as well as the developed standardised test procedures, a prototype of a stationary natural gas-based 2 kW_{el} PEMFC CHP system has been analysed regarding power and optimisation potential. Thereby the most important criteria have been identified influencing the PEMFC CHP system efficiency.

Aside a preferably high fuel utilisation rate the reduction of the auxiliaries electric power consumption is one of the main tasks. By reducing the electrical power consumption down from 400 to 100 W an electrical net efficiency increase up to 3.5% could be achieved.

As well by feeding back the anode offgas to the burner and the optimisation of the reformer insulation noticeable efficiency increases can be achieved. Therefore with the tool it was possible to predict an average absolute efficiency increase of 5% electrical and 3% thermal for the anode offgas recirculation as well a total efficiency increase of 2.45% using a three times better reformer insulation.

Aside these directly the existing system affecting achievements alternative system concepts can lead to better total system efficiencies. For the 2 kW_{el} PEMFC CHP system fuel treatment an alternative concept using a selective methanation instead of a selective oxidation has been simulated. This concept allows a more compact system structure, a reduction or even removal of air treatment and dosing components and a simplification of the thermal system concept. Together with the above-mentioned direct system opti-

misation strategies this leads to possible system net efficiencies of 22% electrical and 35.5% thermal compared to actual 7.7% electrical and 21% thermal. The predicted values are in good agreement with efficiencies of comparable, real pre-commercial systems and prototypes.

The developed modular model-aided system analysis and optimisation environment presented in this work enables an easy and fast optimisation of prototype systems. The tool also allows a detailed characterisation and analysis of systems and components and gives us the possibility for flexible and dynamic simulations in the fast developing process of new systems.

Acknowledgements

The German Federal Ministry of Education and Research (BMBF) is acknowledged for the financial support (FKZ: 03SF0310D; GZ: GIN-SFVF03SF0310D).

References

[1] P. König, A. Weber, N. Lewald, T. Aicher, L. Jörissen, E. Ivers-Tiffée, Fuel Cells 7 (1) (2007) 70–77.
[2] P. König, A. Weber, E. Ivers-Tiffée, ECS Trans. 1 (6) (2005) 453.
[3] P. König, A. Weber, N. Lewald, T. Aicher, L. Jörissen, E. Ivers-Tiffée, R. Szolak, M. Brendel, J. Kaczerowski, J. Power Sources 145 (2) (2005) 327–335.
[4] P. König, H. Timmermann, E. Ivers-Tiffée, Proceedings of the 7th European Solid Oxide Fuel Cell Forum, Lucerne, Switzerland, 2006.
[5] European Commission JRC, FCTESTNET, Fuel Cell Testing and Standardisation Thematic Network, WP2 Stationary Fuel Cell Systems Test Programs and Test Modules, http://fctesqa.jrc.ec.europa.eu/downloads/Stationary/060603%20FCTESTNET%20Stationary%20Applications.pdf, 2006.
[6] European Commission JRC, FCTESQA, Fuel Cell Testing, Safety & Quality Assurance, http://fctesqa.jrc.ec.europa.eu/, http://ie.jrc.ec.europa.eu/fctestnet/, 2006.
[7] J.C. Amphlett, R.F. Mann, B.A. Peppley, P.R. Roberge, A. Rodrigues, J. Power Sources 61 (1996) 183–188.
[8] M.W. Fowler, R.F. Mann, J.C. Amphlett, B.A. Peppley, P.R. Roberge, J. Power Sources 106 (2002) 274–283.
[9] H. Timmermann, A. Weber, U. Hennings, E. Ivers-Tiffée, R. Reimert, Proceedings of the 7th European Solid Oxide Fuel Cell Forum, Lucerne, Switzerland, 2006.
[10] P.W. Atkins, Physikalische Chemie, VCH, Weinheim, 1988.
[11] H.S. Fogler, Elements of Chemical Reaction Engineering, Prentice Hall PTR, Upper Saddle River, NJ, 2002.
[12] W. Vielstich, W. Schmickler, Elektrochemie, Steinkopff, Dietrich, 1976.
[13] R.M. Felder, R.W. Rousseau, Elementary Principles of Chemical Processes, 3rd ed., John Wiley, New York, 2000.
[14] R.C. Reid, The Properties of Gases and Liquids, McGraw-Hill, New York, 1987.
[15] VDI-Gesellschaft Verfahrenstechnik und Chemieingenieurwesen (GVC), VDI-Wärmeatlas, Springer, Berlin, Heidelberg, 1997.
[16] J. Larminie, Fuel Cell Systems Explained, Wiley, Chichester, Weinheim, 2000.
[17] M. Wöhr, Instationäres Thermodynamisches Verhalten Der Polymermembran-Brennstoffzelle, VDI-Verlag, Düsseldorf, 2000.
[18] K. Stephan, F. Mayinger, Thermodynamik, Grundlagen Und Technische Anwendungen, Band 2 Mehrstoffsysteme Und Chemische Reaktionen, Springer, Heidelberg, Berlin, 1999.
[19] W. Vielstich, A. Lamm, H. Gasteiger, Handbook of Fuel Cells: Fundamentals, Technology, Applications, 4-Volume Set, Wiley, New York, 2003.
[20] G. Gummert, Stationäre Brennstoffzellen: Technik Und Markt, Müller, Heidelberg, 2006.
[21] K. Heikrodt, Erdgasbetriebene PEMFC-Hausenergieversorgungsanlage: Innovativer Beitrag Zur Emissions-Und Energiereduktion, VDI-Verlag, Düsseldorf, 2004.
[22] K. Sander, Potenziale Und Perspektiven Stationärer Brennstoffzellen, IER, Stuttgart, 2004.